

# On the Use of ARM Data in the Validation and Refinement of a GCM Radiation Parameterization Scheme

*G. L. Stephens, R. T. Austin, P. M. Gabriel, and N. B. Wood  
Colorado State University  
Department of Atmospheric Science  
Fort Collins, Colorado*

## Introduction

Data provided under the Atmospheric Radiation Measurement (ARM) Program of the U.S. Department of Energy have been analyzed with the goal of evaluating a radiation parameterization scheme currently used in both cloud resolving models and general circulation models (GCMs). These evaluations are also used to develop refinements to the parameterization scheme, and the performance of the climate model has been assessed with these refinements. The specific areas examined include (1) cloud overlap, (2) in-cloud horizontal inhomogeneity, and (3) broadband fluxes and heating rates.

## Cloud Overlap

A large body of composited radar, lidar and ceilometer data from the active remotely sensed cloud layer (ARSCL) locations (Clothiaux et al. 2000) data set have been used to evaluate the cloud overlap treatments used in present GCM radiation schemes (Stephens et al. 2004). Approximately 2000 GCM-like cloud fields (domains) were constructed using twelve months of data sampled from North Slope of Alaska (NSA), Tropical Western Pacific (TWP), and Southern Great Plains (SGP) sites. Within domains, the resolution of the ARSCL data was degraded to 19 vertical layers to match typical GCM resolution, and cloud water mixing ratios were averaged horizontally. Domain-averaged independent column approximation (ICA) calculations, which incorporate the exact cloud overlap, were performed for each domain as were parameterized calculations using five different plane-parallel treatments for cloud overlap. Calculations were made using BUGSrad (Stephens et al. 2001), a two-stream, correlated-K radiative transfer code used in single-column, cloud resolving, and general circulation models. Bias and root mean square (rms) errors for the parameterized calculations were obtained by comparison with the ICA results.

The comparisons reveal a number of deficiencies with the overlap parameterizations. Two commonly-used schemes, random and maximum-random, suffer a severe problem in that the total cloud amount defined by these methods depends on the vertical resolution of the host model. Increasing the number of computational layers into which a cloud is divided increases the total cloud amount. Both of these methods introduce almost negligible bias in the fluxes and heating rates at the 19-layer resolution used here, but the rms errors are large and an inevitable consequence of the parameterization process (Figure 1). The more-commonly used maximum random method does not perform significantly better

than the random method in terms of bias or rms errors despite having a computational cost almost 2.5 times larger.

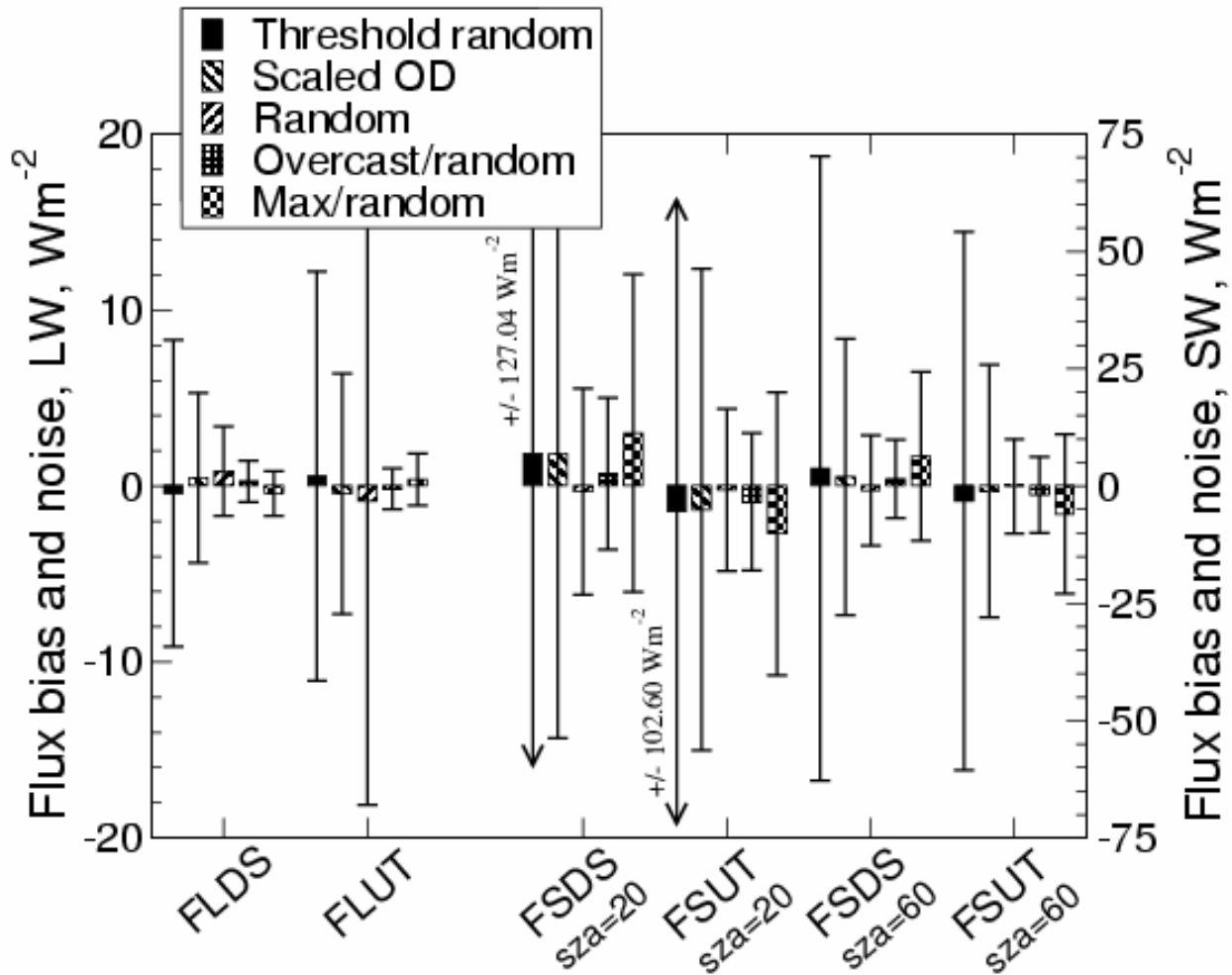


**Figure 1.** The bias and random errors of boundary fluxes associated with the five different overlap schemes. The solar flux errors are shown for the two stated values of the solar zenith angle. The bias errors are indicated by the shaded bars, the rms errors by the extended lines.

A new overlap method is introduced which is efficient, conserves total cloud amount, and can use information about the vertical decorrelation length scales derivable from cloud radar observations. Given total cloud amount, the grid box is divided into three regions: a purely clear-sky region, a purely overcast region, and a randomly overlapped region. The fractional area for each region is adjusted so that total cloud amount is maintained regardless of the number of cloudy layers. Total cloud amount may be provided by the host model, or may be determined using layer cloud fractions and an assumption about decorrelation length. The overcast random method (ORM) has a computational cost equivalent to the random method, making it almost three times faster than the maximum random method. The ORM produced bias and rms errors in exitant fluxes that were significantly smaller than those from all other methods.

## Horizontal Inhomogeneity

For this portion of the work, the role of horizontal inhomogeneity in radiative transfer through cloud fields is investigated (Wood et al. 2004). Using the same ARSCL data used for the work on cloud overlap described above, a new set of GCM-like domains was constructed for which the cloud water mixing ratios were not horizontally averaged. As before, domain-averaged ICA calculations were performed for each domain. In contrast to the previous work, these ICA calculations incorporate the effects of horizontal inhomogeneity in the cloud water mixing ratio fields. Comparisons between ICA calculations with horizontally homogeneous cloud water mixing ratios (from part [1]) and these ICA calculations show that, absent overlap errors, errors caused by treating inhomogeneous cloud fields as homogeneous are significant (Figure 2).

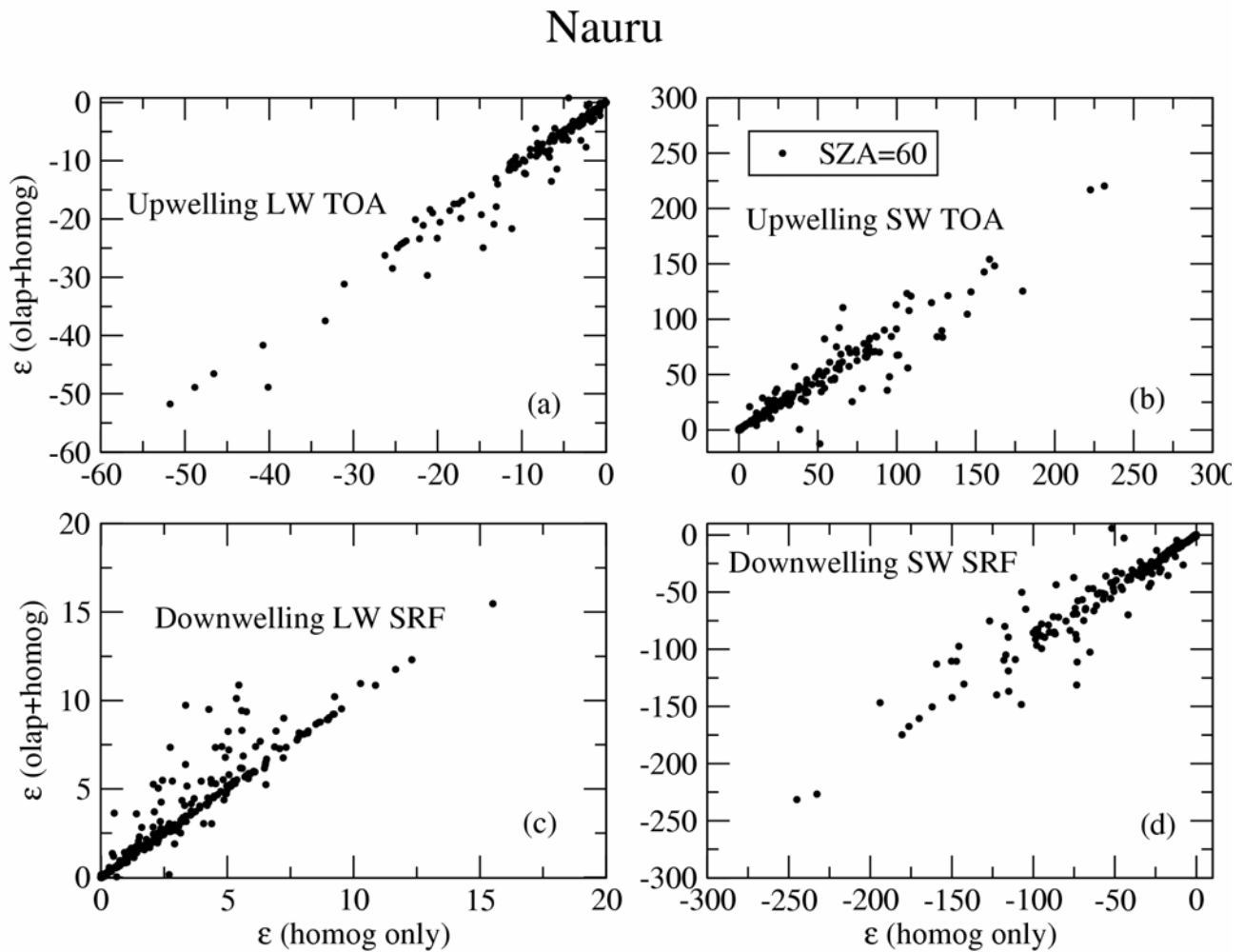


**Figure 2.** Comparison of errors (in  $\text{Wm}^{-2}$ ) due to overlap parameterization plus horizontal homogenization (vertical axes) with those due solely to horizontal homogenization (horizontal axes) for all TWP domains for (a) upwelling longwave flux at top-of-atmosphere, (b) upwelling shortwave flux at top-of-atmosphere, (c) downwelling longwave flux at the surface, and (d) downwelling shortwave flux at the surface. Shortwave fluxes are for a 60-degree solar zenith angle.

To derive a treatment for horizontal inhomogeneity, spatial correlations between cloud optical properties and the radiance field are introduced in the three-dimensional radiative transfer equation and lead to a two-stream model in which the correlations are represented by parameterizations (Stephens 1988). Positive correlations between extinction or scattering and the radiance field are shown to decrease transmission, increase reflection, and in the case of extinction, decrease absorption within inhomogeneous media. Two scalar parameters must be defined for the scheme:  $C_{eI}$ , which defines the spatial correlation between the extinction coefficient and the radiance; and  $C_{sI}$ , which defines the spatial correlation between the scattering coefficient and the radiance. The resulting two-stream radiative transfer model consists of the BUGSrad two-stream model with the ORM treatment for cloud overlap and with longwave and shortwave two-stream solvers modified to incorporate this treatment for in-cloud inhomogeneity.

The ARM data is then applied to calculate representative values for the parameters  $C_{eI}$  and  $C_{sI}$ . For each domain, the parameterized version of BUGSrad is used to perform radiative transfer calculations assuming a range of values for  $C_{eI}$  and  $C_{sI}$ . The results for these calculations are compared with the horizontally-inhomogeneous, domain-averaged ICA calculations. For simplicity, only the exitant radiative fluxes are compared, and the parameter values, which produce the best-fit to the ICA calculations, are determined. The means and standard deviations of the resulting  $C_{eI}$  values are shown in Table 1.

A key facet in the evaluation of the parameterization is its application to the radiative transfer in a GCM. BUGSrad has been implemented in the National Center for Atmospheric Research (NCAR) Community Atmospheric Model (CAM) as part of other work. Two 2-year model integrations were performed, one with the parameterization (the “test” case) and one without (the “control”). Integrations were performed using CAM version 2.0 with seasonally varying fixed climatological sea surface temperatures. The annually-averaged values from the second year of the model run show modifications to the radiative fluxes: enhanced downwelling shortwave flux, a slight decrease in shortwave atmospheric absorption, and increased longwave atmospheric absorption. Because the model runs are performed with prescribed sea surface temperatures, the potential responses of the model are somewhat limited. However, land surface temperatures are free to respond via a coupled land surface mode and adjust to values in the range from +3.7K to -3.5K relative to the control (Figure 3). These results suggest significant regional climatological biases may be introduced into model integrations due to the omission of the treatment of horizontal inhomogeneity.

## **Broadband Fluxes and Heating Rates**

As part of further validation of the BUGSrad radiative transfer model, evaluations are performed on individual cases developed from the March 2000 cloud intensive observation period (IOP) by the Cloud Properties and Broad Band Heating Rate Profile product working groups. These cases represent clear- and cloudy-sky, instantaneous and time-averaged observations over the SGP site, and integrate retrieved cloud microphysical properties (via the MicroBase algorithm) with surface and top-of-atmosphere radiation measurements and with reference radiative transfer model calculations (via the Rapid Radiative Transfer Model, RRTM, which uses an 8-stream DISORT-like radiative transfer algorithm and, like BUGSrad, correlated-K treatment for gas absorption).

**Table 1.** Mean and standard deviation of best-fit  $C_{eI}$  values for each exitant flux and for each ARM site. FSDS is the downwelling shortwave flux at the surface, FSUT is the upwelling shortwave flux at the top of the atmosphere (TOA), FLDS is the downwelling longwave flux at the surface and FLUT is the upwelling longwave flux at the TOA.

		FSDS, sza 20		FSUT, sza 20	
Locale	N	$\overline{C_{eI}}$	$\sigma$	$\overline{C_{eI}}$	$\sigma$
Nauru	640	-0.1392	0.3056	-0.1171	0.3458
SGP Summer	357	-0.2017	0.3767	-0.1342	0.4698
SGP Winter	469	0.09808	0.8513	-0.4264	0.5109
NSA Summer	287	-0.08554	0.5258	-0.1038	0.5852
NSA Winter	252	-0.08373	0.2056	-0.0998	0.2250
		FSDS, sza 60		FSUT, sza 60	
Locale	N	$\overline{C_{eI}}$	$\sigma$	$\overline{C_{eI}}$	$\sigma$
Nauru	640	-0.2305	0.3070	-0.2423	0.3228
SGP Summer	357	-0.2389	0.3697	-0.1826	0.4659
SGP Winter	469	-0.2736	0.3783	-0.2216	0.4749
NSA Summer	287	-0.1556	0.5042	-0.1057	0.5517
NSA Winter	252	-0.1466	0.2111	-0.1248	0.2911
		FLDS		FLUT	
Locale	N	$\overline{C_{eI}}$	$\sigma$	$\overline{C_{eI}}$	$\sigma$
Nauru	640	0.3431	0.6839	-0.02030	0.1684
SGP Summer	357	0.3717	0.7639	-0.0688	0.2938
SGP Winter	469	0.4310	0.8211	-0.0641	0.2857
NSA Summer	287	0.2584	0.8101	-0.00854	0.4521
NSA Winter	252	0.2659	0.8512	0.0367	0.3043

For clear skies, comparisons are made among the instantaneous measurements of the surface fluxes, the reference calculations done with RRTM, and two-stream plane parallel calculations made with BUGSrad. For this work, BUGSrad was modified to incorporate the same aerosol optical properties used by RRTM and to use spectral surface albedos consistent with those used by RRTM. The agreement between BUGSrad and the surface flux measurements was found to be remarkably good. In most of the 36 cases examined, the residual error between BUGSrad and the shortwave measurements was equal to or smaller than that of RRTM (Figure 4). Similar results were achieved for the longwave.

For cloudy skies, comparisons are made between fluxes calculated using RRTM and those calculated using BUGSrad. Both RRTM and BUGSrad used cloud microphysical properties (effective radius and mixing ratio) retrieved by MicroBase. Again, the agreement between RRTM and BUGSrad for the 128 longwave cases and 65 shortwave cases was remarkably good. The residuals versus measurements for BUGSrad were similar to those for RRTM (Table 2), except for the case of the top-of-atmosphere

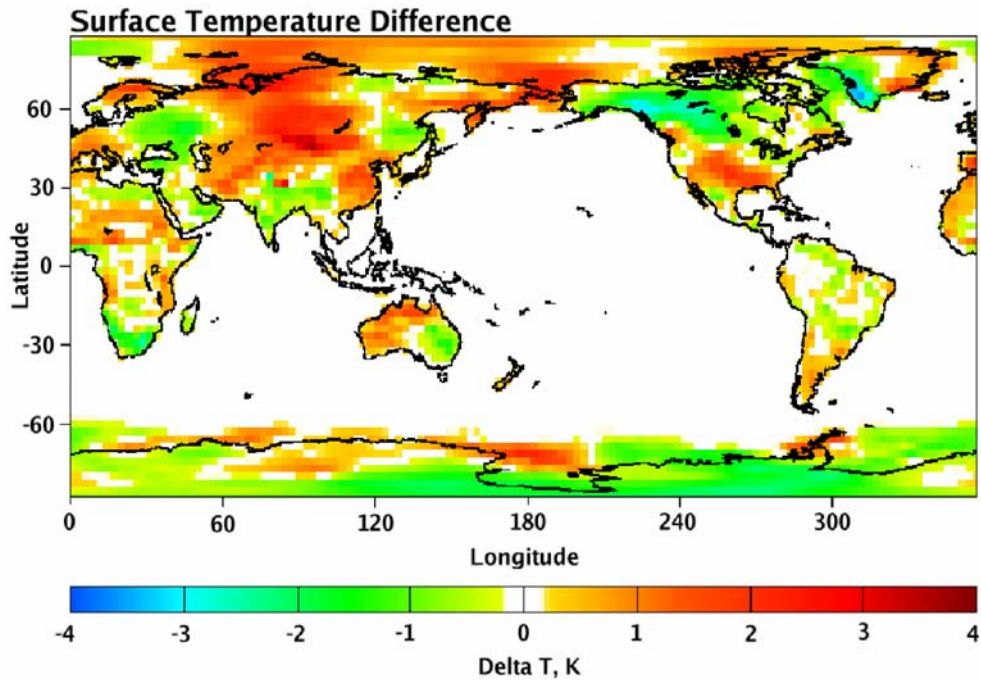


**Figure 3.** Annually-averaged surface temperature differences (test - control) for the second year of a two-year GCM integration for which the test case includes the parameterization for horizontal inhomogeneity in cloud optical properties.

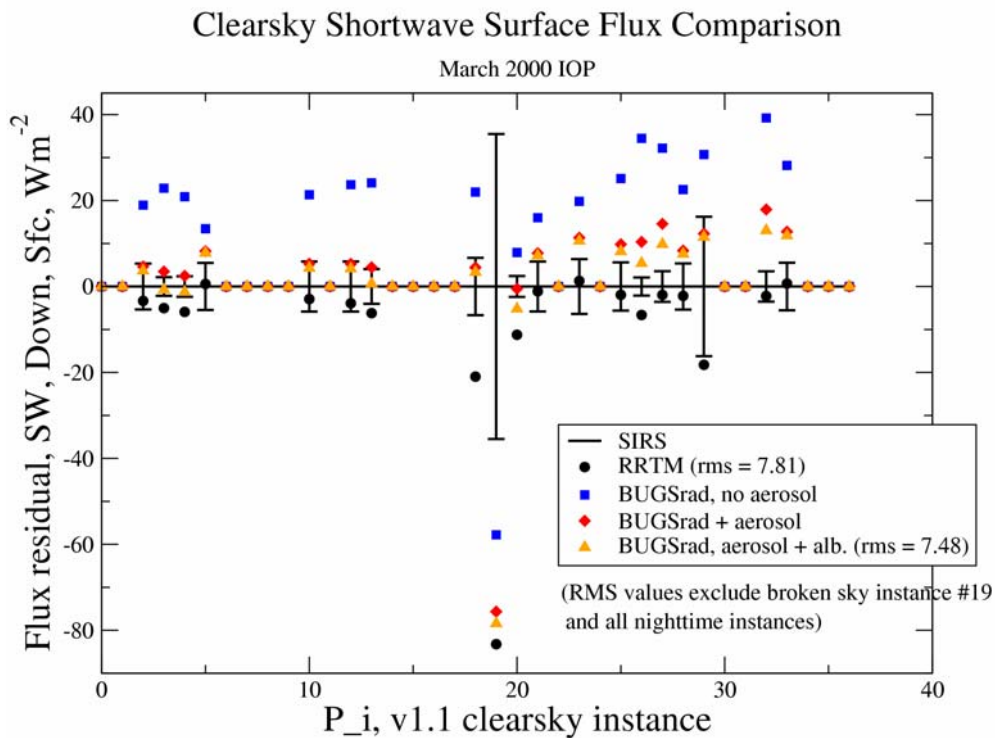


**Figure 4.** Residuals versus measured downwelling shortwave flux at the surface for clear-sky BBHRP cases from the March 2000 IOP. Error bars represent the standard deviation in the measured values.

**Table 2.** Comparison of exitant fluxes for cloudy sky BBHRP cases from the March 2000 IOP. Fluxes are as defined in Table 1 except that FSNT is the net (positive down) shortwave flux at the TOA.

		RRTM	BUGSrad	BUGSrad+CloudSat
$N_{LW}= 128$	$N_{SW}= 65$	$Wm^{-2}$		$(N_{LW}=N_{SW}=8)$
FLUT	Residual Mean (SD)	10.75 (18.52)	10.89 (17.83)	6.68(4.10)
FLDS	Residual Mean (SD)	-3.45 (22.64)	-10.35 (24.89)	-0.61(6.44)
FSNT	Residual Mean (SD)	-77.89 (72.43)	-90.89 (70.82)	-44.36(53.89)
FSDS	Residual Mean (SD)	-28.44 (86.74)	-21.13 (87.44)	34.50(58.25)

net solar flux, where BUGSrad exhibited a somewhat stronger residual than did RRTM ( $-91 Wm^{*-2}$  for BUGSrad versus  $-78 Wm^{*-2}$  for RRTM).

To explore further the issues related to the TOA net solar flux, an alternate retrieval algorithm was applied to obtain cloud microphysical properties for eight of the cloudy sky cases. This alternate algorithm is being used to retrieve cloud liquid water profiles for CloudSat (Stephens et al. 2003) and utilizes visible optical depth data in addition to cloud radar data. Applying the new retrieved values to the BUGSrad calculations significantly reduced the residual in the TOA net solar flux relative to measurements (Table 2, rightmost column), indicating the importance of proper cloud microphysical parameters to such calculations.

## Acknowledgements

This work was supported in part under the U. S. Department of Energy ARM Program Grant DE-FG03-94ER61748 and in part under National Science Foundation Grant ATM-0120149. Data was provided by the ARM Program sponsored by the U. S. Department of Energy, Office of Science, Office of Biological and Environmental Research, Environmental Sciences Division. Thanks to Mark Miller, Eli Mlawer, and Tim Shippert for assistance with MicroBase and BBHRP data; to Qilong Min for providing optical depth data.

## Corresponding Author

Norman Wood, [norm@atmos.colostate.edu](mailto:norm@atmos.colostate.edu), (970) 491-8480

## References

Clothiaux, E. E., T. P. Ackerman, G. G. Mace, K. P. Moran, R. T. Marchand, M. A. Miller, and B. E. Martner, 2000: Objective determination of cloud heights and radar reflectivities using a combination of active remote sensors at the ARM CART sites. *J. Appl. Meteorol.*, **49**, 645–665.

Stephens, G. L., 1988: Radiative transfer through arbitrarily shaped optical media. Part II: Group theory and simple closures. *J. Atmos. Sci.*, **45**, 1837–1848.

Stephens, G. L., P. T. Partain, and P. M. Gabriel, 2001: Parameterization of atmospheric radiative transfer. Part I: Validity of Simple Models. *J. Atmos. Sci.*, **48**, 3391–3409.

Stephens, G. L., et al., 2003: The CloudSat mission and the A-Train: A new dimension of space-based observations of clouds and precipitation. *Bull. Amer. Met. Soc.*, **83**, 1771–1790.

Stephens, G. L., N. B. Wood, and P. M. Gabriel, 2004: An assessment of the parameterization of subgrid-scale cloud effects on radiative transfer. Part I: Vertical Overlap. *J. Atmos. Sci.*, **61**, 715–732.

Wood, N. B., P. M. Gabriel, and G. L. Stephens, 2004: An assessment of the parameterization of subgrid-scale cloud effects on radiative transfer. Part II: Horizontal inhomogeneity, in preparation.